

Random phase approximation with second-order screened exchange for current-carrying atomic states

Wuming Zhu, 1,a) Liang Zhang, 2 and S. B. Trickey 3,a)

¹Department of Physics, Hangzhou Normal University, 16 Xuelin Street, Hangzhou, Zhejiang 310036, China ²Institute of Service Engineering, Hangzhou Normal University, 2318 Yuhangtang Road, Cangqian, Hangzhou, Zhejiang 311121, China

³Quantum Theory Project, Department of Physics and Department of Chemistry, University of Florida, P.O. Box 118435, Gainesville, Florida 32611-8435, USA

(Received 9 September 2016; accepted 22 November 2016; published online 13 December 2016)

The direct random phase approximation (RPA) and RPA with second-order screened exchange (SOSEX) have been implemented with complex orbitals as a basis for treating open-shell atoms. Both RPA and RPA+SOSEX are natural implicit current density functionals because the paramagnetic current density implicitly is included through the use of complex orbitals. We confirm that inclusion of the SOSEX correction improves the total energy accuracy substantially compared to RPA, especially for smaller-Z atoms. Computational complexity makes post self-consistent-field (post-SCF) evaluation of RPA-type expressions commonplace, so orbital basis origins and properties become important. Sizable differences are found in correlation energies, total atomic energies, and ionization energies for RPA-type functionals evaluated in the post-SCF fashion with orbital sets obtained from different schemes. Reference orbitals from Kohn-Sham calculations with semi-local functionals are more suitable for RPA+SOSEX to generate accurate total energies, but reference orbitals from exact exchange (non-local) yield essentially energetically degenerate open-shell atom ground states. RPA+SOSEX correlation combined with exact exchange calculated from a hybrid reference orbital set (half the exchange calculated from exact-exchange orbitals, the other half of the exchange from orbitals optimized for the Perdew-Burke-Ernzerhof (PBE) exchange functional) gives the best overall performance. Numerical results show that the RPA-like functional with SOSEX correction can be used as a practical implicit current density functional when current effects should be included. Published by AIP Publishing. [http://dx.doi.org/10.1063/1.4971377]

I. INTRODUCTION

The random phase approximation (RPA)¹ long has been valuable for the development of approximate density functionals. Early on, the RPA correlation energy of the homogeneous electron gas was used in fitting analytical forms of local density approximations (LDAs) for exchange and correlation (XC).²⁻⁴ RPA expressions also were used to determine the density gradient dependence and shape of correlation holes.^{5,6} RPA and related functionals utilize both occupied and unoccupied orbitals, hence stand on the fifth rung of the Jacob's ladder of approximate functional complexity. Fully compatible with exact-exchange, they show promise to solve several long-standing difficulties with less sophisticated C approximations, hence have attracted much attention in recent years. As RPA overestimates short-range correlation, 8 it also has been used in conjunction with short-ranged local or semilocal density functionals, thereby combining the strengths of both. 9-13 Recently, many RPA variants and so-called beyond-RPA methods have been devised. Successful applications to atoms, molecules, surfaces, and solids have been reported. 14-18 Some recent reviews on RPA are given in Refs. 19–21.

In the broader context of XC functional development, there is a common limitation. Most conventional approximate XC functionals fail to yield a properly degenerate ground state energy for current-carrying and zero-current states of openshell atoms.^{22,23} Ayers and Levy have given constraints on XC functionals for delivering such degenerate states and observed that it is very difficult to imagine a semi-local functional (e.g., generalized gradient approximation, GGA and meta-GGA, mGGA) which would be able to meet those constraints.²⁴ But even exact exchange treated approximately (occupied orbitals only in the optimized effective potential) fails to give proper degeneracy in the spin-unrestricted case.^{25,26} The usual diagnosis attributes the failure to the lack of paramagnetic current density dependence in the approximate functionals. Multiple remedies have been proposed^{27–30} based upon modification of existing functionals, either by introducing explicit current dependence or doing so implicitly through complex orbitals.

The form of explicit current-dependent modifications is ambiguous: there is no plain prescription for how a current density should be added to those functionals. Guidance might be sought from the more general case of an applied external magnetic field. In principle, that requires invocation of current density functional theory (CDFT).³¹ Vignale and Rasolt gave a gauge-invariance argument that CDFT XC functionals should depend upon the so-called vorticity,



a) Authors to whom correspondence should be addressed. Electronic addresses: zhuwm@hznu.edu.cn and trickey@qtp.ufl.edu

$$v(\mathbf{r}) \equiv \nabla \times \frac{\mathbf{j}_p(\mathbf{r})}{n(\mathbf{r})}.$$
 (1)

Here $\mathbf{j}_{n}(\mathbf{r})$ is the paramagnetic current density and $n(\mathbf{r})$ is the electron number density. Vignale, Rasolt, and Geldart proposed a local approximation for the current contribution to the XC energy denoted as VRG. 31,32 Unfortunately, our previous studies on both Hooke's atom and real atoms showed that ν is a difficult computational variable, VRG can be qualitatively wrong, and inclusion of ν -dependence did not lead to systematic improvement^{33,34} in the quality of computed results. Orestes et al. 35,36 side-stepped this problem by using perturbative CDFT expressions for the orbital susceptibility to calculate ionization energies. While they found current-induced lowering of states, they did not find resolution of the degeneracy breaking. Roughly concurrently, Tao and Perdew extended the vorticity-dependent correction to GGA and mGGA XC functionals²⁹ directly. Though the result for degeneracy breaking was substantial improvement for both types of approximate functional, full degeneracy was not restored. The nature of the problem subsequently was illustrated by explicit construction of a non-spherical potential which was constrained to recover the required degeneracy.³⁷

The great majority of density functional theory (DFT) calculations use the Kohn-Sham (KS) decomposition to produce KS orbitals via self-consistent field (SCF) iterations. In the case of so-called lower-rung functionals, the orbitals are used only in generating $n(\mathbf{r})$, its density gradient (for use in GGA XC functionals), and the kinetic energy density (for use in mGGAs). An implicit common assumption is that \mathbf{j}_p contributions are small, hence are ignorable. When they are non-negligible, CDFT requires that the auxiliary KS system must generate the same $n(\mathbf{r})$ and \mathbf{j}_p as for the real system.³¹ For non-zero \mathbf{j}_p , complex KS orbitals therefore are essential; real orbitals always yield vanishing current. Thus, for example, Ref. 28 remarks on the use of complex linear combinations in the PBE functional.

As noted, there has been recent progress on higherrung, orbital-dependent functionals, with accuracy and performance gains in many situations³⁸ relative to the GGA and mGGA functionals. Use of complex orbitals in an orbitaldependent functional naturally defines an implicit CDFT functional, because of implicit dependence upon both $n(\mathbf{r})$ and \mathbf{j}_n . This observation seems to have originated with Pittalis et al., who treated only occupied orbitals in their Krieger-Li-Iafrate (KLI) approximation²⁶ treatment of degeneracy breaking in exact exchange.²⁵ Subsequently they also considered orbitaldependence in the Colle-Salvetti C functional as evaluated from those exact-exchange (KLI approximation) orbitals.³⁰ Again this is an occupied-orbital case. The spurious splittings were reduced but not eliminated. A perhaps questionable aspect is that the Colle-Salvetti functional is extracted from a non-N-representable model density matrix.³⁹

RPA-like functionals are, at present, the most elaborate orbital-dependent functional class. Though not specifically designed for including current effects, their successes 19-21

make it worthwhile to investigate whether they become effective CDFT functionals to describe systems with non-vanishing \mathbf{j}_p simply via evaluation with complex orbitals. In view of the fundamental importance of the degeneracy-breaking issue, here we use free atoms, including those with open shells, to examine RPA-like functionals and their capabilities for predicting accurate atomic total energies, and ionization energies (IP), as well as describing degenerate ground states.

Essential formulations are given in Sec. II, including basis sets and numerical methods, followed by results and discussion in Section III, and a concluding summary in Section IV.

II. METHODOLOGY

As in the case of other rather complicated XC functionals, in this study the RPA-like functionals were implemented in post-SCF fashion, that is, with a set of reference orbitals obtained from a local or semi-local XC approximation or from a Hartree-Fock (HF) calculation. We comment briefly on this procedure in Sec. IV.

A. Basics

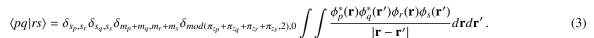
The single-particle orbitals of an atom at the origin are expanded in Gaussian-type basis functions contracted from primitives χ_i expressed in cylindrical coordinates (ρ, z, ϕ) ,

$$\chi_j(\rho, z, \phi) = N_j \rho^{n_{\rho_j}} z^{n_{z_j}} e^{-\alpha_j \rho^2 - \beta_j z^2} e^{im_j \phi}, j = 1, 2, 3, \dots,$$
(2)

where N_j is the normalization coefficient, $n_{\rho_j} = |m_j| + 2k_j$, $k_j = 0, 1, \ldots$, with magnetic quantum number $m_j = \ldots, -2$, $-1, 0, 1, 2, \ldots$, and $n_{z_j} = \pi_{z_j} + 2l_j, l_j = 0, 1, \ldots$, with z-parity $\pi_{z_j} = 0, 1$. This type of basis functions has the flexibility to describe the effects of an external magnetic field on an atom by the use of different transverse and longitudinal exponents α_j and β_j . The present study, however, considered only free atoms without an external field, so we used $\alpha_j = \beta_j$. Both contraction coefficients and basis exponents were obtained from the correlation-consistent basis sets of Dunning. As an aside, note that the use of real spherical harmonics would not yield KS states that are eigenfunctions of \hat{L}_z .

Upon numerical convergence of the SCF KS calculation, the non-interacting KS kinetic energy T_s , Hartree energy J (classical electron-electron repulsion), and nuclear-electron potential energy E_{ne} are available, along with occupied and unoccupied KS spin orbitals, in shorthand notation $p = \phi_p(\mathbf{r}, \sigma)$, and corresponding eigenvalues ϵ_p . As usual, indices i, j, \ldots denote occupied orbitals, a, b, \ldots denote virtual orbitals, and p, q, \ldots denote any orbitals. \mathbf{r} and $\sigma = \uparrow, \downarrow$ are space and spin coordinates. A HF calculation yields the analogous HF quantities, so in the ensuing discussion we refer only to KS unless necessary.

When KS orbitals are expanded in complex basis functions centered at the origin, Eq. (2), all the two-electron integrals are real, since each orbital p has a definite magnetic quantum number m_p ,



Thus $\langle pq|rs \rangle = \langle qp|sr \rangle = \langle rs|pq \rangle = \langle sr|qp \rangle$, but note that $\langle pq|rs \rangle \neq \langle ps|rq \rangle$, unlike the case for real orbitals. Only required, non-zero electron integrals are stored and transformed in our implementation. From the occupied KS orbitals, \mathbf{j}_p is

$$\mathbf{j}_{p}(\mathbf{r},\sigma) = \frac{1}{2i} \sum_{i}^{occ} \left[\phi_{i}^{*}(\mathbf{r},\sigma) \nabla \phi_{i}(\mathbf{r},\sigma) - \phi_{i}(\mathbf{r},\sigma) \nabla \phi_{i}^{*}(\mathbf{r},\sigma) \right]. \tag{4}$$

Exact-exchange in DFT is defined as the Fock integral evaluated with occupied KS orbitals,

$$E_x^{XX} = -\frac{1}{2} \sum_{i,j}^{occ} \langle ij | ji \rangle.$$
 (5)

A combination of exact-exchange E_x^{XX} with TPSS correlation,⁴¹ which yields good performance for atoms over a large range of magnetic field strengths,³⁴ also is included for comparison,

$$E_{xc}^{HGGA} = E_x^{XX} + E_c^{TPSS}. (6)$$

Since E_x^{XX} is fully non-local, this combination corresponds to the fourth rung of the XC Jacob's ladder or hyper-GGA (HGGA).⁷ Cautions regarding this combination were mentioned earlier.³⁴

B. RPA details

Here we give essential details of construction of the RPA correlation energy in the case of complex orbitals, a more or less straightforward generalization of the real-orbital case. ^{13,42} The RPA correlation energy is expressed in spin-orbitals via a coupling-constant integral as

$$E_{c}^{RPA} = \frac{1}{2} \int_{0}^{1} d\lambda \sum_{ia,jb} \left\{ \langle ib|aj \rangle \sum_{n} \left[(\mathbf{X}_{n,\lambda})_{ia}^{*} (\mathbf{X}_{n,\lambda})_{jb} + (\mathbf{Y}_{n,\lambda})_{ia}^{*} (\mathbf{Y}_{n,\lambda})_{jb} - \delta_{ij} \delta_{ab} \right] + \langle ij|ab \rangle \sum_{n} \left[(\mathbf{X}_{n,\lambda})_{ia}^{*} (\mathbf{Y}_{n,\lambda})_{jb} + (\mathbf{Y}_{n,\lambda})_{ia}^{*} (\mathbf{X}_{n,\lambda})_{jb} \right] \right\},$$
(7)

with the same orbital indexing convention as used before. λ is the coupling constant introduced in the adiabatic connection formula. $(\mathbf{X}_{n,\lambda}, \mathbf{Y}_{n,\lambda})$ are the solutions of the linear-response non-Hermitian eigenvalue equation,

$$\begin{pmatrix} \mathbf{A}_{\lambda} & \mathbf{B}_{\lambda} \\ \mathbf{B}_{\lambda}^{*} & \mathbf{A}_{\lambda}^{*} \end{pmatrix} \begin{pmatrix} \mathbf{X}_{n,\lambda} \\ \mathbf{Y}_{n,\lambda} \end{pmatrix} = \omega_{n,\lambda} \begin{pmatrix} \mathbf{1} & \mathbf{0} \\ \mathbf{0} & -\mathbf{1} \end{pmatrix} \begin{pmatrix} \mathbf{X}_{n,\lambda} \\ \mathbf{Y}_{n,\lambda} \end{pmatrix}. \tag{8}$$

The eigenvector normalization is chosen as $\mathbf{X}_{n,\lambda}^{\dagger}\mathbf{X}_{m,\lambda}$ $-\mathbf{Y}_{n,\lambda}^{\dagger}\mathbf{Y}_{m,\lambda}=\delta_{nm}$. The so-called orbital rotation Hessians \mathbf{A}_{λ} and \mathbf{B}_{λ} have the matrix elements,

$$(\mathbf{A}_{\lambda})_{ia,ib} = (\epsilon_a - \epsilon_i)\delta_{ij}\delta_{ab} + \lambda \langle ib|aj\rangle, \tag{9a}$$

$$(\mathbf{B}_{\lambda})_{ia\ ib} = \lambda \langle ab|ij \rangle,\tag{9b}$$

where ϵ_i and ϵ_a are the KS orbital eigenvalues.

For real orbitals, the foregoing expressions can be simplified further by using $\langle ib|aj\rangle = \langle ij|ab\rangle$, ^{13,42} but here we must evaluate Eq. (7) with complex KS spin orbitals. Since all the

two-electron integrals are real, $\mathbf{A}_{\lambda}^* = \mathbf{A}_{\lambda}$ and $\mathbf{B}_{\lambda}^* = \mathbf{B}_{\lambda}$. The combinations $\mathbf{A}_{\lambda} \pm \mathbf{B}_{\lambda}$ appear throughout the development. $(\mathbf{A}_{\lambda} - \mathbf{B}_{\lambda})$ is positive definite on grounds of the Aufbau prinzip, while $(\mathbf{A}_{\lambda} + \mathbf{B}_{\lambda})$ is a positive-definite Coulomb integral at all proper coupling strengths. The supermatrix equation (8) reduces to

$$(\mathbf{A}_{\lambda} \pm \mathbf{B}_{\lambda}) (\mathbf{X}_{n,\lambda} \pm \mathbf{Y}_{n,\lambda}) = \omega_{n,\lambda} (\mathbf{X}_{n,\lambda} \mp \mathbf{Y}_{n,\lambda}). \tag{10}$$

Upon introduction of the one-component vectors,

$$\mathbf{Z}_{\pm,n,\lambda} = \omega_{n,\lambda}^{1/2} (\mathbf{A}_{\lambda} \mp \mathbf{B}_{\lambda})^{-1/2} (\mathbf{X}_{n,\lambda} \pm \mathbf{Y}_{n,\lambda}), \qquad (11)$$

the non-Hermitian eigenvalue equation (10) is transformed to two half-sized eigenvalue equations, namely,

$$\mathbf{M}_{\pm,\lambda} \mathbf{Z}_{\pm,n,\lambda} = \omega_{n\,\lambda}^2 \mathbf{Z}_{\pm,n,\lambda} \,. \tag{12}$$

Here $\mathbf{M}_{\pm,\lambda} = (\mathbf{A}_{\lambda} \mp \mathbf{B}_{\lambda})^{1/2} (\mathbf{A}_{\lambda} \pm \mathbf{B}_{\lambda}) (\mathbf{A}_{\lambda} \mp \mathbf{B}_{\lambda})^{1/2}$. The spectral decomposition $\mathbf{M}_{\pm,\lambda}^{-1/2} = \sum_{n} \omega_{n,\lambda}^{-1} \mathbf{Z}_{\pm,n,\lambda}^{\mathbf{Z}} \mathbf{Z}_{\pm,n,\lambda}^{\mathbf{T}}$, then enables the RPA C energy to be expressed as

$$E_c^{RPA} = \frac{1}{4} \int_0^1 d\lambda \sum_{ia,jb} \left\{ \langle ib|aj \rangle \left[(\mathbf{P}_{+,\lambda})_{ia,jb} + (\mathbf{P}_{-,\lambda})_{ia,jb} \right] \right\}$$

$$+ \langle ij|ab\rangle \left[(\mathbf{P}_{+,\lambda})_{ia,jb} - (\mathbf{P}_{-,\lambda})_{ia,jb} \right] , \qquad (13)$$

where

$$\mathbf{P}_{\pm,\lambda} = (\mathbf{A}_{\lambda} \mp \mathbf{B}_{\lambda})^{1/2} \mathbf{M}_{\lambda}^{-1/2} (\mathbf{A}_{\lambda} \mp \mathbf{B}_{\lambda})^{1/2} - \mathbf{1}. \tag{14}$$

As a consequence of Eq. (3), the summation over occupied-virtual spin orbital pairs in Eq. (13) can be decomposed by spin $i = i \uparrow, i \downarrow$ and simplified to $\sum_{ia,jb} = (\sum_{i\uparrow a\uparrow} + \sum_{i\downarrow a\downarrow})(\sum_{j\uparrow b\uparrow} + \sum_{j\downarrow b\downarrow})$.

The RPA functional defined thereby often is called direct RPA (dRPA) or simply RPA. Since the Coulomb integrals used in the expressions are not antisymmetrized, the direct-RPA C energy suffers from electron self-interaction error (SIE). One way to remove the one-electron self-correlation in RPA is to add the second-order screened exchange (SOSEX) correction. That scheme is called RPA+SOSEX. 43,44 Its C expression is obtained by replacing the two-electron Coulomb integrals in Eq. (13) by their anti-symmetrized counterparts, to wit

$$E_c^{RPA+SOSEX} = \frac{1}{4} \int_0^1 d\lambda \sum_{ia\,ib} \left\{ \langle ib \parallel aj \rangle \left[(\mathbf{P}_{+,\lambda})_{ia,jb} + (\mathbf{P}_{-,\lambda})_{ia,jb} \right] \right\}$$

$$+ \langle ij \parallel ab \rangle \left[(\mathbf{P}_{+,\lambda})_{ia,jb} - (\mathbf{P}_{-,\lambda})_{ia,jb} \right] \right\}, \tag{15}$$

where $\langle ib \parallel aj \rangle = \langle ib \mid aj \rangle - \langle ia^* \mid b^*j \rangle$, $\langle ij \parallel ab \rangle = \langle ij \mid ab \rangle - \langle ij \mid ba \rangle$, and a^*, b^* are the complex conjugates of virtual orbitals a and b, respectively. With a little algebra, one obtains the spin-decomposed SOSEX correction to RPA,

$$E_{c}^{RPA+SOSEX} = E_{c}^{RPA} - \frac{1}{4} \int_{0}^{1} d\lambda \Biggl(\sum_{i\uparrow a\uparrow, j\uparrow b\uparrow} + \sum_{i\downarrow a\downarrow, j\downarrow b\downarrow} \Biggr)$$

$$\times \Biggl\{ \langle ia^{*}|b^{*}j\rangle \left[(\mathbf{P}_{+,\lambda})_{ia,jb} + (\mathbf{P}_{-,\lambda})_{ia,jb} \right]$$

$$+ \langle ij|ba\rangle \left[(\mathbf{P}_{+,\lambda})_{ia,jb} - (\mathbf{P}_{-,\lambda})_{ia,jb} \right] \Biggr\}. \quad (16)$$

All the coupling-constant integrations in Eqs. (13) and (16) can be performed with suitable accuracy by a 7-point

Gauss-Legendre quadrature.⁴² Correlation-consistent polarized core-valence basis sets, cc-pCVXZ, of Dunning were used.⁴⁰ Here X = 3,4,5 is a cardinal number. Since the RPA C energy exhibits slow convergence with respect to basis set size,⁴⁵ we extrapolated these to the complete basis set (CBS) limit $E_c(CBS)$ using a two-point extrapolation scheme.

$$E_c(X) = E_c(CBS) + \frac{C}{X^3}.$$
 (17)

It is assumed that C is a constant for a given atom and family of correlation-consistent basis sets that differ only by cardinal numbers X. Except for the Li and Be atoms and their ions, for which we used X = 3,4, we used X = 4,5 extrapolation. Self-consistent DFT and HF energies from local or semi-local functionals were extrapolated to the CBS limit with a three-point exponential formula,

$$E^{DFT/HF}(X) = E^{DFT/HF}(CBS) + Ae^{-BX}, \qquad (18)$$

where X = 3, 4, 5.46

III. RESULTS AND DISCUSSION

First we consider neutral atoms with nuclear charge $Z \le 18$, including eight open p-shell atoms. Closed shell atoms and those with a half-filled p-shell (N and P) have ground states with no current density and total atomic magnetic

quantum number $M_L = 0$. Atoms with one electron in their open outer p-shell (B, O, Al, S) can have either the p_0 orbital occupied, rendering $\mathbf{j}_p = 0$ and $M_L = 0$, or either the p_+ or p_- orbital occupied, resulting in non-zero current density and $M_L = \pm 1$. For two p-electrons in the open shell (C, F, Si, Cl), the electronic configuration p_+p_- corresponds to $M_L = 0$ (zero-current), and configurations p_+p_0 and p_0p_- correspond to $M_L = \pm 1$ (non-vanishing \mathbf{j}_p).

Because both RPA and RPA+SOSEX calculations were implemented non-self-consistently ("post-SCF"), it is necessary to note both the approximation and the reference SCF orbital set used for its evaluation. We follow the notation introduced by Ren *et al.* to label a chosen correlation method and its reference orbital set. 21,47 For example, RPA+SOSEX@PBE means RPA correlation energy with SOSEX correction evaluated with self-consistent orbitals from a calculation that used PBE XC. In this study, RPA-like functionals always were combined with exact exchange E_x^{XX} and the same reference orbital set was used for both X and C unless explicitly stated otherwise.

In Tables I and II, we give correlation energies and atomic total energy deviations from experimental values ($E_{calculated} - E_{expt}$) calculated from several different functionals. For self-consistent DFT calculations, two approximate functionals, PBE⁴⁹ and TPSS, are included as representatives of GGA- and mGGA-tier functionals. The HGGA

TABLE I. Correlation energy in atoms from SCF-DFT, RPA, and RPA+SOSEX methods. KS orbitals are from PBE, TPSS, and exchange-only functionals (energy in Hartree).

	SCF-	DFT ^b		RPA @		RPA+S0	OSEX @	
Atom ^a	PBE	TPSS	PBE	TPSS	EXX ^c	PBE	TPSS	Expt.d
Не	-0.0411	-0.0427	-0.0843	-0.0825	-0.083	-0.0422	-0.0413	-0.042 044
Li	-0.0510	-0.0496	-0.1117	-0.1100	-0.112	-0.0448	-0.0441	-0.045 33
Be	-0.0854	-0.0874	-0.1813	-0.1764	-0.179	-0.0921	-0.0896	-0.094 34
$B(M_L=0)$	-0.1125	-0.1149	-0.2376	-0.2279		-0.1152	-0.1114	-0.12485
$B(M_L = 1)$	-0.1146	-0.1172	-0.2310	-0.2252		-0.1192	-0.1163	
$C(M_L = 0)$	-0.1438	-0.1475	-0.2934	-0.2839		-0.1438	-0.1404	-0.156 40
$C(M_L = 1)$	-0.1459	-0.1496	-0.2846	-0.2784		-0.1477	-0.1446	
N	-0.1785	-0.1835	-0.3392	-0.3328	-0.335	-0.1768	-0.1738	-0.188 31
$O(M_L = 0)$	-0.2326	-0.2361	-0.4330	-0.4227		-0.2391	-0.2350	-0.257 94
$O(M_L = 1)$	-0.2349	-0.2388	-0.4241	-0.4176		-0.2452	-0.2415	
$F(M_L=0)$	-0.2888	-0.2923	-0.5254	-0.5151		-0.3074	-0.3033	-0.324 53
$F(M_L = 1)$	-0.2912	-0.2951	-0.5142	-0.5075		-0.3138	-0.3096	
Ne	-0.3464	-0.3504	-0.6052	-0.5982	-0.597	-0.3808	-0.3765	-0.39047
Na	-0.3687	-0.3705	-0.6279	-0.6214	-0.626	-0.3881	-0.3839	-0.395 64
Mg	-0.4091	-0.4142	-0.6898	-0.6823	-0.687	-0.4334	-0.4286	-0.438 28
$Al(M_L = 0)$	-0.4442	-0.4485	-0.7539	-0.7433		-0.4639	-0.4583	-0.469 60
$Al(M_L = 1)$	-0.4452	-0.4499	-0.7505	-0.7426		-0.4674	-0.4627	
$Si(M_L = 0)$	-0.4831	-0.4880	-0.8101	-0.7989		-0.4955	-0.4902	-0.505 03
$Si(M_L = 1)$	-0.4844	-0.4894	-0.8055	-0.7971		-0.4991	-0.4944	
P	-0.5249	-0.5308	-0.8599	-0.8511	-0.850	-0.5324	-0.5275	-0.540 26
$S(M_L = 0)$	-0.5830	-0.5877	-0.9464	-0.9341		-0.5881	-0.5817	-0.604 76
$S(M_L = 1)$	-0.5850	-0.5904	-0.9432	-0.9334		-0.5950	-0.5892	
$Cl(M_L = 0)$	-0.6431	-0.6478	-1.0327	-1.0195		-0.6498	-0.6433	-0.665 98
$Cl(M_L = 1)$	-0.6450	-0.6503	-1.0281	-1.0179		-0.6570	-0.6506	
Ar	-0.7045	-0.7096	-1.1082	-1.0976	-1.101	-0.7160	-0.7094	-0.722 16

 $^{^{}a}M_{L} = 1$ for current-carrying atomic ground states, and $M_{L} = 0$ for ground states with no paramagnetic current.

dExperimental estimate of correlation energy. Data from Ref. 48.



^bSelf-consistent field DFT calculations with GGA (PBE XC functional) and meta-GGA (TPSS XC functional).

^cSelf-consistent exact exchange only orbitals. Data from Ref. 14.

TABLE II. Deviations of total atomic energies by different methods from experimental estimates (energy in Hartree).

	SCF-DFT ^b						RPA+SOSEX @						
Atom ^a	PBE	TPSS	HGGA ^c	-Fock	PBE	TPSS	HGGA ^c	HF	Hyb. 1 ^d	Hyb. 2 ^e	Expt.f		
Не	0.010	-0.006	-0.001	0.042	0.001	0.002	0.008	0.008	-0.011	-0.005	-2.903 72		
Li	0.016	-0.011	-0.004	0.045	0.003	0.002	0.009	0.007	-0.008	-0.003	-7.478 06		
Be	0.038	-0.004	0.007	0.094	0.005	0.006	0.030	0.027	-0.002	0.001	-14.667 36		
$B(M_L=0)$	0.042	-0.015	0.006	0.121	0.011	0.012	0.034	0.034	-0.008	0.001	-24.653 91		
$B(M_L = 1)$	0.046	-0.005	0.006	0.124	0.008	0.010	0.034	0.034	-0.006	0.001	-24.6539		
$C(M_L = 0)$	0.046	-0.022	0.003	0.151	0.015	0.015	0.038	0.038	-0.015	-0.000	-37.845 0		
$C(M_L = 1)$	0.050	-0.013	0.003	0.154	0.012	0.013	0.039	0.038	-0.013	-0.000	-37.845 0		
N	0.053	-0.027	-0.001	0.184	0.016	0.016	0.040	0.039	-0.023	-0.003	-54.5892		
$O(M_L = 0)$	0.052	-0.043	0.010	0.248	0.021	0.021	0.052	0.052	-0.029	-0.004	-75.0673		
$O(M_L = 1)$	0.061	-0.024	0.010	0.252	0.017	0.018	0.052	0.051	-0.029	-0.006	-75.0673		
$F(M_L = 0)$	0.057	-0.047	0.021	0.317	0.024	0.024	0.061	0.060	-0.038	-0.007	-99.7339		
$F(M_L = 1)$	0.066	-0.031	0.022	0.321	0.020	0.021	0.061	0.060	-0.037	-0.009	-99.7339		
Ne	0.070	-0.045	0.035	0.390	0.025	0.025	0.068	0.066	-0.048	-0.012	-128.9376		
Na	0.082	-0.043	0.023	0.396	0.017	0.018	0.060	0.060	-0.031	-0.007	-162.2546		
Mg	0.098	-0.041	0.022	0.438	0.014	0.016	0.068	0.067	-0.025	-0.005	-200.053		
$Al(M_L = 0)$	0.110	-0.042	0.015	0.465	0.012	0.014	0.066	0.065	-0.030	-0.009	-242.346		
$Al(M_L = 1)$	0.113	-0.036	0.017	0.468	0.011	0.012	0.066	0.065	-0.025	-0.007	-242.346		
$Si(M_L = 0)$	0.125	-0.041	0.011	0.500	0.013	0.017	0.072	0.071	-0.028	-0.007	-289.359		
$Si(M_L = 1)$	0.127	-0.036	0.012	0.503	0.012	0.015	0.072	0.072	-0.023	-0.006	-289.359		
P	0.144	-0.036	0.007	0.540	0.023	0.018	0.078	0.077	-0.020	0.002	-341.259		
$S(M_L = 0)$	0.157	-0.038	0.008	0.597	0.023	0.023	0.089	0.088	-0.024	-0.001	-398.110		
$S(M_L = 1)$	0.162	-0.030	0.010	0.602	0.020	0.020	0.089	0.088	-0.020	-0.000	-398.110		
$Cl(M_L = 0)$	0.174	-0.036	0.009	0.658	0.021	0.023	0.097	0.096	-0.024	-0.001	-460.148		
$Cl(M_L = 1)$	0.177	-0.029	0.011	0.664	0.018	0.020	0.098	0.097	-0.021	-0.001	-460.148		
Ar	0.194	-0.029	0.011	0.723	0.018	0.020	0.103	0.102	-0.021	-0.002	-527.540		
Average	0.091	-0.029	0.011	0.360	0.015	0.016	0.059	0.059	-0.022	-0.004			

 $^{^{}a}M_{L}$ = 1 for current-carrying atomic ground states, and M_{L} = 0 for ground states with no paramagnetic current.

combination of exact-exchange E_x^{XX} with TPSS correlation, Eq. (6), also is included.

Our spherical atom results can be compared with published data from SCF-PBE and RPA calculations. Our PBE total energies differ from those in Ref. 50 by no more than 0.3 mH except for Ne, for which we obtained an energy 1.5 mH lower. The reason for this discrepancy is uncertain but plausibly reflects a difference in basis sets (and, perhaps, in CBS) extrapolation procedures). For open-shell atoms, we always get energies a few mH below those in Ref. 50 because a nonspherical electron density is admissible in our calculation. Our RPA energies can be compared to the data from the work of Jiang and Engel. ¹⁴ For RPA@PBE, the total atomic energies agree with their RPA@BLYP data within 1 mH, except for two noble gas atoms, Ne (ours is 4 mH higher) and Ar (ours is 4 mH lower). Again, the difference may arise from basis sets or reference orbital sets. For example, we used CBS extrapolation whereas they used a hard-wall cavity approach. The generally nice agreement shows overall good convergence in our calculations however.

Jiang and Engel commented that the RPA energies are insensitive to reference orbitals, ¹⁴ but we find that to depend

a bit on the energy standard used. We take the standard to be that differences larger than 2 mH (≈1.25 kcal/mol) are consequential. Consider what happens with PBE and TPSS (two non-empirical XC functionals in the same lineage) as generators of reference orbital sets. RPA correlation energies based on their orbitals differ appreciably, especially for open-shell atoms. This difference clearly is discernible in Table I. For the Cl atom with no current, the E_c^{RPA} difference is as large as 13 mH, albeit the total energy difference is somewhat smaller, only 8 mH. The RPA correlation energies based on exact-exchange orbitals from Ref. 14 also are given in Table I for comparison. Typically those values are between our E_c^{RPA} results from RPA@PBE and RPA@TPSS. Janesko and Scuseria also have reported as much as a 50% shift in E_c from range-separated RPA depending upon whether the reference orbitals arose from semi-local or non-local exchange.11

This sensitivity of RPA-like functionals may be valuable as well, in the sense that more orbital detail is detected by the functionals. The specific case most related to this study is that E_c^{RPA} and $E_c^{RPA+SOSEX}$ can recognize the two degenerate ground states of open-shell atoms with different current



^bSelf-consistent field DFT calculations with GGA (PBE XC functional), meta-GGA (TPSS XC functional), and HGGA (exact exchange functional and TPSS correlation functional, see Eq. (6)).

^cHyper-generalized gradient approximation. Chosen functionals are exact exchange and TPSS correlation functional.

^dHybrid references. Exact exchange energy from HF orbitals and other pieces of energy from PBE orbitals.

eHybrid references. Half of the exact exchange energy from HF orbitals and the other half from PBE orbitals. Other pieces of energy from PBE orbitals. See Eq. (19). This column is actually the average of the two columns labeled by PBE and Hyb. 1 under the category RPA+SOSEX.

^fExperimental estimate of total atomic energy. Data from Ref. 48.

As is well known by now, RPA grossly overestimates the magnitude of atomic correlation energies.⁹ The situation is much improved by adding the SOSEX correction. This aspect is seen clearly in Table I. For smaller Z atoms, $E_c^{RPA+SOSEX}$ has nearly halved E_c^{RPA} , with less dramatic reduction in magnitude for larger Z atoms. The dependence of the correlation energy on reference orbitals also is reduced nearly by half but still is discernible. Inclusion of the SOSEX correction removes electron self-interaction (SI) in correlation, with the result being a C functional fully compatible with E_x^{XX} , and correspondingly improved C energies. Understandably, SI is more severe in few-electron systems and thus the SOSEX correction to RPA is more significant for smaller Z atoms. In fact, semi-local functionals, PBE and TPSS, themselves give rather accurate C energies for the higher Z atoms. From Table I one sees that $E_c^{RPA+SOSEX}$ @PBE improves E_c^{PBE} considerably, but $E_c^{RPA+SOSEX}$ @TPSS does not improve much over E_c^{TPSS} , an indication that much of the RPA excitation contribution has been incorporated properly in the TPSS C functional. For atoms with $Z \ge 5$, although $E_c^{RPA+SOSEX}$ is very close to experimental values, it is still nearly 10 mH short. This is perhaps because of the absence of single excitations in RPA-like functionals.47

As to atomic total energies, Table II shows that PBE systematically gives under-estimates and TPSS systematically gives over-estimates. The HGGA combination, Eq. (6), improves upon both of them significantly. Since direct RPA without correction gives atomic energies that are too low, E^{RPA} is not included in Table II. RPA+SOSEX@PBE and RPA+SOSEX@TPSS results are very close to one another, with no obvious improvement over self-consistent HGGA energies. There is no meaningful dependence of RPA+SOSEX total atomic energies on PBE versus TPSS orbitals (both from semi-local functionals). But the use of non-local HGGA or HF orbitals instead gives quite large changes. This again shows the importance of choosing suitable reference orbitals for post-SCF evaluation of RPA-like functionals. It appears that orbitals from semi-local functionals are the better choice for total energies.

Since RPA omits single excitation, Ren *et al.* proposed a hybrid-RPA scheme as an approximate remedy. In it, HF orbitals are used for E_x^{XX} and PBE orbitals for E_c^{RPA} .⁴⁷ We also checked this hybrid scheme in our RPA+SOSEX calculation. Results from it are labeled as "Hyb. 1" in Table II. It does not improve upon RPA+SOSEX@PBE total energies but shifts their error from positive to negative. We thus tried a new

scheme, labeled as "Hyb. 2" in Table II, namely,

$$E_{xc}^{Hyb.2} = \frac{1}{2} \left(E_x^{XX} @HF + E_x^{XX} @PBE \right) + E_c^{RPA+SOSEX} @PBE$$
(19)

in which only half of E_{χ}^{XX} is calculated from HF orbitals, with the other half still calculated from PBE orbitals. This combination is the average of RPA+SOSEX@PBE and RPA+SOSEX@Hyb. 1. It gives very accurate atomic total energies, with an average error of only 4 mH. The combination is reminiscent of the earlier half-exact-exchange hybrid approach proposed by Becke.⁵¹ Details of how these two prescriptions are related remain for subsequent investigation.

Now we turn to the long-existing difficulty of nondegeneracy of current-carrying atomic configurations (M_L = ± 1) and zero-current configurations ($M_L = 0$) summarized at the outset.²³ Since local and semi-local functionals usually generate lower energies for $M_L = 0$, that value commonly is chosen as the ground state. Table III compiles the differences in total energies between $M_L = \pm 1$ and $M_L = 0$ states from a variety of computational prescriptions. Our data in the SCF-PBE column agree precisely with those from Ref. 28 because their construction of complex KS orbitals is equivalent to ours. However, our SCF-PBE and SCF-TPSS energy splittings are consistently larger than those given in Ref. 29. Apparently the difference stems primarily from the different reference orbital sets employed. While we use non-spherical self-consistent orbitals, Tao and Perdew used spherical spinrestricted HF orbitals and densities.

Next we consider various schemes to remove the spurious energy splittings between current-carrying and zero-current atomic ground state densities. In Table III, Becke's modification of the Becke-Roussel functional²⁷ is labeled as jBR. The spurious splittings are reduced significantly but not removed. The extension of PBE by Maximoff, Ernzerhof, and Scuseria²⁸ to include \mathbf{j}_p explicitly is labeled as jPBE. Table III shows that it can give smaller magnitude splittings than does iBR, but not consistently so. That table also includes the findings of Ref. 25, namely, that the exact-exchange-only functional in the KLI approximation²⁶ gives much larger magnitude splittings in spin-unrestricted calculations than in the spinrestricted case. Those results are listed under the headings x-KLI, subheading SDFT for spin-unrestricted DFT, subheading DFT for spin-restricted. The SDFT splittings are roughly 10% smaller than HF splittings.

Results from the Tao-Perdew²⁹ extension of both GGA and mGGA functionals to include dependence upon the gauge-invariant vorticity variable ν , yielding functionals called CGGA and CMGGA, respectively, are listed in Table III under the heading ν -DFT. They reduce the artificial splittings in their parent functionals by more than half but their performance is not as impressive as the \mathbf{j}_p -dependent functionals.

In that context, it is significant that Table III shows that self-consistent HGGA itself reduces the spurious splittings substantially, by four-fold from PBE and eight-fold from TPSS. RPA+SOSEX@PBE only decreases the PBE splitting by half, but the order of degenerate ground states is reversed. Current-carrying states ($M_L = \pm 1$) have lower energies than

TABLE III. Total atomic energy differences $\Delta E = E(M_L = \pm 1) - E(M_L = 0)$ (energy in kcal/mol) for open-shell atoms from different methods.

	SCF-DFT ^a		Hartree	RPA+SOSEX @						jDFT ^b		ν –DFT c		x-KLI ^d		
Atom	PBE	TPSS	HGGA ^e	-Fock	PBE	TPSS	HGGAe	HF	Hyb.1 ^f	Hyb.2 ^g	jBR ^h	jPBE ⁱ	CGGA	CMGGA	SDFT	DFT
В	2.89	6.71	0.06	1.81	-1.37	-0.82	0.13	0.06	1.69	0.16	0.61	0.10	1.19	2.51	1.66	0.06
C	2.73	5.60	0.20	1.76	-1.40	-1.32	0.13	0.00	1.53	0.07	0.38	-0.20	1.26	2.26	1.58	0.06
O	6.05	11.87	0.40	2.51	-2.03	-1.95	-0.50	-0.25	0.25	-0.89	0.92	-0.70	1.82	3.89	2.36	0.55
F	5.48	9.61	0.61	2.56	-2.15	-2.07	0.06	0.00	0.60	-0.78	0.66	-0.70	2.38	3.77	2.32	0.40
Al	1.74	3.59	0.86	1.90	-1.02	-1.19	0.19	0.13	3.27	1.13	0.23	0.30	0.06	0.69	1.68	0.04
Si	1.26	2.92	1.04	2.04	-0.86	-1.00	0.31	0.25	2.77	0.96	0.00	-0.10	0.19	0.82	1.76	0.05
S	2.84	5.00	1.26	3.34	-2.03	-1.88	0.19	-0.06	2.56	0.27	0.12	0.20	-0.13	0.38	3.04	0.34
Cl	2.18	4.09	1.62	3.42	-2.11	-1.69	0.44	0.25	2.07	-0.02	0.01	-0.20	0.88	1.78	3.15	0.25
Mean	3.15	6.17	0.76	2.42	-1.62	-1.49	0.12	0.05	1.84	0.11	0.37	-0.16	0.96	2.01	2.19	0.22
MAE	3.15	6.17	0.76	2.42	1.62	1.49	0.24	0.13	1.84	0.53	0.37	0.31	0.99	2.01	2.19	0.22

^aSelf-consistent field DFT calculations with GGA (PBE XC functional), meta-GGA (TPSS XC functional), and HGGA (exact exchange functional and TPSS correlation functional, see Eq. (6)).

zero-current states ($M_L = 0$) in the RPA+SOSEX@PBE calculation. Since TPSS has large splittings, it is perhaps unsurprising that RPA+SOSEX@TPSS reduces those greatly but leaves unsatisfactory results nevertheless. RPA+SOSEX@HGGA and RPA+SOSEX@HF, which are not the best performers for atomic total energies, give the smallest mean splittings and the smallest mean absolute errors (MAEs) among all the methods included in Table III. It may be important for the reference orbitals to be self-interaction free in order for RPA+SOSEX to be able to predict degenerate ground states. Results from RPA+SOSEX calculations based on hybrid orbital sets discussed above also are included in Table III. Perhaps the hybrid scheme 2 is the best choice when both the accuracy of total energy and the near-degeneracy of different ground states are taken as simultaneous requirements.

Alternatively, one may examine atomic ionization energies. On the basis of their finding only small but non-negligible current-dependent effects, Orestes *et al.*^{35,36} suggested that functional refinement was required. With higher-rung functionals now available, especially orbital-dependent ones which can include current density naturally provided that complex orbitals are used, it is reasonable to restudy the issue. Therefore we also checked the first atomic ionization energies produced from the different methods studied in this work.

The ionization energy (IP) was taken as the difference between the free atom total energy and that of its corresponding singly positive ion. As before, there is an ambiguity for some atoms in the calculated ionization energy, namely, whether a current-carrying or zero-current state is chosen for the neutral atom and for the ion. Table IV therefore shows explicitly the chosen atomic and ionic states used to deduce the IPs reported there. Note that since the two outer p-electrons in the $M_L = 0$ atomic state occupy both the

 p_{+} and the p_{-} orbitals, removing either electron will result in a current-carrying ion, hence the case $M_L = 0 \rightarrow M_L = 0$ is not included in the table. Table IV shows that semi-local functionals actually are not bad for ionization energies. PBE and TPSS again give results close to each other, with their mean absolute errors (MAEs) only 0.2 eV. The use of exact exchange in HGGA reduces the average error but does not improve the MAE. Without SOSEX correction, RPA@PBE results in larger errors than those from either PBE or TPSS. This again traces to the RPA overestimation of correlation energy magnitude (recall Table I and discussion of it). The situation is much improved when the SOSEX correction is added, especially for lower Z atoms. RPA+SOSEX@PBE gives an average error of only -0.06 eV and MAE of 0.08 eV. The use of hybrid reference orbital sets does not yield much gain in accuracy of computed IPs, but the use of the prescription of Eq. (19) does reduce the IP ambiguity substantially. For example, the difference between $C(M_L = 0) \rightarrow C^+(M_L = 1)$ and $C(M_L = 1) \to C^+(M_L = 0)$ is 0.30 eV from PBE, 0.67 eV from TPSS, and 0.63 eV from RPA@PBE, but only 0.01 eV from Eq. (19).

The ambiguity in calculated IPs makes the comparison with experimental data somewhat murky. If one compares the TPSS value for $C(M_L=1) \rightarrow C^+(M_L=0)$ (11.21 eV) to the experimental estimate (11.26 eV), it would seem that the theoretical prediction is quite accurate. However, if one uses the TPSS value for $C(M_L=0) \rightarrow C^+(M_L=1)$ (11.88 eV), the presumed error would increase by an order of magnitude. The ambiguity ultimately limits the predictive power and usefulness of the functional. This embarrassment is largely removed by the use of Eq. (19) since it reduces the ambiguity to a level usually much smaller than other residual errors in calculated IPs. It appears that the effect of current density has been included appropriately in this functional. This



^bExplicit current-dependent DFT functionals.

^cExplicit vorticity-dependent functionals. Data from Ref. 29.

dExact exchange only functional defined by KLI (Krieger-Li-Iafrate) approximation. SDFT for spin-unrestricted and DFT for spin-restricted orbitals. Data from Ref. 25.

^eHyper-generalized gradient approximation. Chosen functionals are exact exchange and TPSS correlation functional.

^fHybrid references. Exact exchange energy from HF orbitals and other pieces of energy from PBE orbitals.

gHybrid references. Half of the exact exchange energy from HF orbitals and the other half from PBE orbitals. Other pieces of energy from PBE orbitals. See Eq. (19). This column is actually the average of the two columns labeled by PBE and Hyb. 1 under the category RPA+SOSEX.

^hData from Ref. 27.

ⁱData from Ref. 28.

TABLE IV. First atomic ionization energies from different methods (energy in eV).

	Ionic configuration ^a		SCF-DFT	b	Hartree	RPA@ PBE	RPA+SOSEX @			
Atomic configuration ^a		PBE	TPSS	HGGA	-Fock		PBE	Hyb. 1 ^c	Hyb. 2 ^d	Expt.e
Li	Li ⁺	5.59	5.51	5.44	5.34	6.02	5.37	5.32	5.35	5.39
Be	Be ⁺	9.00	9.06	9.00	8.04	9.60	9.25	9.15	9.20	9.32
$B(M_L = 1)$	B^+	8.55	8.48	8.62	7.97	8.57	8.30	8.50	8.40	8.30
$B(M_L = 0)$	B^+	8.68	8.77	8.62	8.04	8.80	8.24	8.57	8.40	8.30
$C(M_L = 1)$	$C^+(M_L = 0)$	11.43	11.21	11.50	10.72	11.31	11.28	11.48	11.38	11.26
$C(M_L = 1)$	$C^+(M_L = 1)$	11.61	11.63	11.50	10.81	11.65	11.20	11.54	11.37	11.26
$C(M_L = 0)$	$C^+(M_L = 1)$	11.73	11.88	11.51	10.89	11.94	11.14	11.60	11.37	11.26
N	$N^+(M_L = 1)$	14.89	14.99	14.69	13.98	14.98	14.45	14.98	14.71	14.53
N	$N^+(M_L = 0)$	14.73	14.67	14.69	13.89	14.56	14.52	14.92	14.72	14.53
$O(M_L = 1)$	O_{+}	13.81	13.53	13.21	11.92	13.88	13.55	14.01	13.78	13.62
$O(M_L = 0)$	O_{+}	14.07	14.05	13.23	12.02	14.20	13.46	14.02	13.74	13.62
$F(M_L = 1)$	$F^+(M_L = 0)$	17.43	17.02	16.87	15.54	17.38	17.37	17.93	17.65	17.42
$F(M_L = 1)$	$F^+(M_L = 1)$	17.75	17.67	16.88	15.66	17.83	17.28	17.94	17.61	17.42
$F(M_L = 0)$	$F^+(M_L = 1)$	17.99	18.09	16.91	15.77	18.21	17.18	17.97	17.58	17.42
Ne	$Ne^+(M_L = 1)$	21.95	21.99	20.94	19.77	22.03	21.37	22.26	21.82	21.56
Ne	$Ne^+(M_L=0)$	21.67	21.49	20.91	19.65	21.52	21.47	22.24	21.86	21.56
Na	Na ⁺	5.36	5.18	5.06	4.95	5.64	5.11	5.05	5.08	5.14
Mg	Mg^+	7.61	7.55	7.43	6.61	8.02	7.66	7.48	7.57	7.65
$Al(M_L = 1)$	Al ⁺	6.00	5.99	6.13	5.53	6.36	5.94	5.92	5.93	5.98
$Al(M_L = 0)$	Al ⁺	6.08	6.14	6.16	5.61	6.50	5.90	6.06	5.98	5.98
$Si(M_L = 1)$	$\mathrm{Si}^+(\mathrm{M}_L=0)$	8.14	8.08	8.26	7.55	8.37	8.19	8.00	8.09	8.15
$Si(M_L = 1)$	$Si^+(M_L = 1)$	8.23	8.27	8.32	7.65	8.57	8.13	8.14	8.14	8.15
$Si(M_L = 0)$	$Si^+(M_L = 1)$	8.28	8.39	8.36	7.74	8.76	8.09	8.26	8.18	8.15
P	$P^+(M_L = 1)$	10.54	10.64	10.71	10.01	10.71	10.33	10.54	10.44	10.49
P	$P^+(M_L = 0)$	10.48	10.50	10.65	9.90	10.45	10.38	10.42	10.40	10.49
$S(M_L = 1)$	S^+	10.30	10.24	10.27	9.09	10.65	10.27	10.43	10.35	10.36
$S(M_L = 0)$	S^+	10.43	10.45	10.33	9.24	10.84	10.18	10.54	10.36	10.36
$Cl(M_L = 1)$	$Cl^+(M_L = 0)$	12.87	12.77	12.86	11.61	13.07	13.00	12.93	12.96	12.97
$Cl(M_L = 1)$	$Cl^+(M_L = 1)$	13.01	13.02	12.93	11.78	13.32	12.91	13.05	12.98	12.97
$Cl(M_L = 0)$	$Cl^+(M_L = 1)$	13.10	13.20	13.00	11.92	13.55	12.81	13.14	12.98	12.97
Ar	$Ar^+(M_L = 1)$	15.80	15.88	15.83	14.71	16.18	15.82	15.94	15.88	15.76
Ar	$Ar^+(M_L=0)$	15.70	15.69	15.75	14.55	15.88	15.92	15.84	15.88	15.76
Avera	0.15	0.12	-0.05	-0.93	0.35	-0.06	0.19	0.06		
Mean abs	0.18	0.21	0.24	0.93	0.36	0.08	0.24	0.10		

 $^{^{\}mathrm{a}}$ Atom and ion electronic configurations. $M_L=1$ for current-carrying ground states and $M_L=0$ for ground states with no paramagnetic current.

good feature also is found in the HGGA functional, see Eq. (6).

IV. SUMMARY AND CONCLUSIONS

From the study of total atomic energies, spurious splittings between current-carrying and zero-current atomic states, and ionization potentials, we find that two functionals are the best in their overall performance. One is E_x^{XX} combined with TPSS correlation, which stands on the HGGA rung of the DFT functional hierarchy ladder. It has the virtue of simplicity while providing sizable improvement over semi-local functionals. Although RPA+SOSEX@PBE has rather good performance and gives very accurate atomic ionization energies, the spurious splittings from this functional between two

degenerate atomic ground states, $M_L = 0$ and $M_L = 1$, still are too large to be acceptable. The use of hybrid reference orbital sets, Eq. (19), incorporates the current density and considerably reduces spurious splitting, while simultaneously giving highly accurate atomic total energies and ionization energies. This functional is the other one that we propose to use at the fifth rung of the ladder. It is plausibly a practical implicit current density functional one could use when current effects need to be included.

Given the context, it is almost automatic to raise the question of whether there are explicit CDFT functionals (current or vorticity-dependent) which could be useful in conjunction with the orbital-dependent functionals evaluated with complex orbitals. One obvious form of such a strategy would be to obtain the SCF orbitals from such an explicit CDFT



^bSelf-consistent field DFT calculations with GGA (PBE XC functional), meta-GGA (TPSS XC functional), and HGGA (exact exchange functional and TPSS correlation functional, see Eq. (6)).

^cHybrid references. Exact exchange energy from HF orbitals and other pieces of energy from PBE orbitals.

^dHybrid references. Half of the exact exchange energy from HF orbitals and the other half from PBE orbitals. See Eq. (19). This column is actually the average of the two nearest columns to the left.

^eExperimental estimate of atomic ionization energy. Data from Ref. 48.

functional calculation (instead of, for example, a PBE XC calculation). The barrier to this approach, as we discussed in the Introduction (see just after Eq. (1)), is that there are no really successful CDFT XC functionals. Earlier we had shown^{33,34} that VRG,³² the only functional available even at the LDA rung of the Jacob's ladder, is unrealistic and that the vorticity is a difficult computational variable. Lack of progress in overcoming those barriers was, in fact, a significant motivation for the present study. Orbital-dependent functionals (e.g., RPA+SOSEX) with complex orbitals appear to alleviate, at the very least, the necessity of including explicit current or vorticity dependence.

ACKNOWLEDGMENTS

Helpful discussions with A. Savin (CNRS), X.-Y. Pan (Ningbo University), Xinguo Ren (USTC), and Jian Wang (Huzhou University) are acknowledged. This work was funded by the Zhejiang Provincial Natural Science Foundation of China under Grant No. LY13A050002 (W. Zhu and L. Zhang), in part by the National Natural Science Foundation of China Grant Nos. 11474081 and 11274085 (W. Zhu), and in part by the U.S. Department of Energy Grant No. DE-SC-0002139 (S. B. Trickey).

- ¹D. Bohm and D. Pines, Phys. Rev. **92**, 609 (1953); P. Noziéres and D. Pines, *ibid.* **111**, 442 (1958).
- ²U. von Barth and L. Hedin, J. Phys. C 5, 1629 (1972).
- ³S. H. Vosko, L. Wilk, and M. Nusair, Can. J. Phys. **58**, 1200 (1980).
- ⁴J. P. Perdew and Y. Wang, Phys. Rev. B **45**, 13244 (1992).
- ⁵D. C. Langreth and J. P. Perdew, Phys. Rev. B **21**, 5469 (1980).
- ⁶Y. Wang and J. P. Perdew, Phys. Rev. B **44**, 13298 (1991).
- ⁷J. P. Perdew and K. Schmidt, AIP Conf. Proc. **577**, 1 (2001).
- ⁸ K. S. Singwi, M. P. Tosi, R. H. Land, and A. Sjölander, Phys. Rev. 176, 589 (1968).
- S. Kurth and J. P. Perdew, Phys. Rev. B 59, 10461 (1999); Z. Yan,
 J. P. Perdew, and S. Kurth, *ibid.* 61, 16430 (2000); A. Ruzsinszky, J. P. Perdew, and G. I. Csonka, J. Chem. Theory Comput. 6, 127 (2010).
- ¹⁰B. G. Janesko, T. M. Henderson, and G. E. Scuseria, J. Chem. Phys. 130, 081105 (2009); 131, 034110 (2009).
- ¹¹B. G. Janesko and G. E. Scuseria, J. Chem. Phys. **131**, 154106 (2009); Erratum **138**, 019901 (2013).
- 12 J. Toulouse, I. C. Gerber, G. Jansen, A. Savin, and J. G. Ángyán, Phys. Rev. Lett. 102, 096404 (2009); W. Zhu, J. Toulouse, A. Savin, and J. G. Ángyán, J. Chem. Phys. 132, 244108 (2010); J. Toulouse, W. Zhu, A. Savin, G. Jansen, and J. G. Ángyán, *ibid.* 135, 084119 (2011).
- ¹³J. Toulouse, W. Zhu, J. G. Ángyán, and A. Savin, Phys. Rev. A 82, 032502 (2010)
- ¹⁴H. Jiang and E. Engel, J. Chem. Phys. **127**, 184108 (2007).
- ¹⁵M. Hellgren and U. von Barth, Phys. Rev. B **76**, 075107 (2007).

- ¹⁶M. Fuchs, Y. M. Niquet, X. Gonze, and K. Burke, J. Chem. Phys. 122, 094116 (2005).
- ¹⁷J. F. Dobson and J. Wang, Phys. Rev. Lett. **82**, 2123 (1999).
- ¹⁸J. Harl and G. Kresse, Phys. Rev. Lett. **103**, 056401 (2009); J. Harl, L. Schimka, and G. Kresse, Phys. Rev. B **81**, 115126 (2010).
- ¹⁹A. Heßelmann and A. Görling, Mol. Phys. **108**, 359 (2010).
- ²⁰H. Eshuis, J. E. Bates, and F. Furche, Theor. Chem. Acc. **131**, 1084 (2012).
- ²¹J. Paier, X. Ren, P. Rinke, G. E. Scuseria, A. Grüneis, G. Kresse, and M. Scheffler, New J. Phys. **14**, 043002 (2012); X. Ren, P. Rinke, C. Joas, and M. Scheffler, J. Mater. Sci. **47**, 7447 (2012).
- ²²J. Dobson, J. Chem. Phys. **98**, 8870 (1993).
- ²³E. J. Baerends, V. Branchadell, and M. Sodupe, Chem. Phys. Lett. **265**, 481 (1997).
- ²⁴P. W. Ayers and M. Levy, J. Chem. Phys. **140**, 18A537 (2014).
- ²⁵S. Pittalis, S. Kurth, and E. K. U. Gross, J. Chem. Phys. **125**, 084105 (2006).
- ²⁶J. B. Krieger, Y. Li, and G. J. Iafrate, *Phys. Rev. A* **45**, 101 (1992).
- ²⁷A. Becke, J. Chem. Phys. **117**, 6935 (2002).
- ²⁸S. Maximoff, M. Ernzerhof, and G. E. Scuseria, J. Chem. Phys. **120**, 2105 (2004).
- ²⁹ J. Tao and J. P. Perdew, Phys. Rev. Lett. **95**, 196403 (2005).
- ³⁰S. Pittalis, S. Kurth, S. Sharma, and E. K. U. Gross, J. Chem. Phys. **127**, 124103 (2007).
- ³¹G. Vignale and M. Rasolt, Phys. Rev. Lett. **59**, 2360 (1987); Phys. Rev. B **37**, 10685 (1988).
- ³²G. Vignale, M. Rasolt, and D. J. W. Geldart, Adv. Quantum Chem. 21, 235 (1990)
- ³³W. Zhu and S. B. Trickey, J. Chem. Phys. **125**, 094317 (2006).
- ³⁴W. Zhu, L. Zhang, and S. B. Trickey, *Phys. Rev. A* **90**, 022504 (2014).
- ³⁵E. Orestes, T. Marcasso, and K. Capelle, Phys. Rev. A **68**, 022105 (2003).
- ³⁶E. Orestes, A. B. F. Silva, and K. Capelle, Int. J. Quantum Chem. 103, 516 (2005).
- ³⁷A. N. Narita, J. Phys. Soc. Jpn. **77**, 124303 (2008).
- ³⁸S. Kümmel and L. Kronik, Rev. Mod. Phys. **80**, 3 (2008).
- ³⁹R. C. Morrison, Int. J. Quantum Chem. **46**, 583 (1993).
- ⁴⁰T. H. Dunning, J. Chem. Phys. **90**, 1007 (1989); D. E. Woon and T. H. Dunning, *ibid*. **103**, 4572 (1995); K. A. Peterson and T. H. Dunning, *ibid*. **117**, 10548 (2002).
- ⁴¹ J. Tao, J. P. Perdew, V. N. Staroverov, and G. E. Scuseria, Phys. Rev. Lett. 91, 146401 (2003).
- ⁴²F. Furche, Phys. Rev. B **64**, 195120 (2001).
- ⁴³D. L. Freeman, Phys. Rev. B **15**, 5512 (1977).
- ⁴⁴A. Grüneis, M. Marsman, J. Harl, L. Schimka, and G. Kresse, J. Chem. Phys. **131**, 154115 (2009).
- ⁴⁵H. Eshuis and F. Furche, J. Chem. Phys. **136**, 084105 (2012).
- ⁴⁶For the He atom, we use cc-pvXz basis sets to extrapolate. For Li and Be atoms, cc-pv5z basis sets are unavailable, and it is assumed RPA and RPA+SOSEX $E_c(CBS)$ from X=3, 4 and X=4, 5 extrapolations are close. HF and DFT total energies of Li and Be are not extrapolated, instead cc-pvqz results are used.
- ⁴⁷X. Ren, A. Tkatchenko, P. Rinke, and M. Scheffler, Phys. Rev. Lett. **106**, 153003 (2011).
- ⁴⁸S. J. Chakravorty, S. R. Gwaltney, E. R. Davidson, F. A. Parpia, and C. F. Fischer, Phys. Rev. A 47, 3649 (1993).
- ⁴⁹J. P. Perdew, K. Burke, and M. Ernzerhof, Phys. Rev. Lett. **77**, 3865 (1996); Erratum **78**, 1396 (1997).
- ⁵⁰U. Argaman, G. Makov, and E. Kraisler, Phys. Rev. A **88**, 042504 (2013).
- ⁵¹A. Becke, J. Chem. Phys. **98**, 1372 (1993).

